ISSN 1070-3632, Russian Journal of General Chemistry, 2014, Vol. 84, No. 10, pp. 1893–1898. © Pleiades Publishing, Ltd., 2014.
Original Russian Text © A.A. Burovikhina, M.V. Chislov, I.A. Rodionov, D.A. Porotnikov, I.A. Zvereva, 2014, published in Zhurnal Obshchei Khimii, 2014, Vol. 84, No. 10, pp. 1612–1617.

Photocatalytic Activity and Intercalation of Layered Perovskite-Like Tantalates $ANdTa_2O_7$ (A = H, Li, Na, K, Rb, Cs)

A. A. Burovikhina, M. V. Chislov, I. A. Rodionov, D. A. Porotnikov, and I. A. Zvereva

St. Petersburg State University, Universitetskii pr. 26, St. Petersburg, 198504 Russia
e-mail: irina.zvereva@spbu.ru

Received April 28, 2014

Abstract—Layered perovskite-like oxides $ANdTa_2O_7$ (A = H, Li, Na, K, Rb, Cs) were synthesized and characterized by means of diffuse reflection spectroscopy, thermogravimetry, and simultaneous thermal and X-ray phase analysis. Comparative analysis of the photocatalytic activity of $ANdTa_2O_7$ in the UV-induced hydrogen evolution from an aqueous isopropanol solution was performed. $NaNdTa_2O_7$ and $HNdTa_2O_7$ are able to intercalate water to the interlayer space. The compositions and thermal stability ranges of intercalates were determined. No explicit correlation between the photocatalytic activity of layered oxides and their ability to intercalate water to the interlayer space was found.

Keywords: layered oxides, perovskite-like oxides, photocatalysis, intercalation

DOI: 10.1134/S1070363214100041

Light-induced decomposition of water is one of the methods of transformation of solar energy for its accumulation as hydrogen — an environmentally safe fuel.

There are several reasons to consider perovskite-like oxides as promising photocatalysts. The high mobility of interlayer cations allows one to widely vary the composition of such compounds [1] and thus affect their optical properties, electronic structure, and photocatalytic activity [2–9]. Certain layered oxides are capable of reversible water intercalation into their interlayer space [2, 6]. This increases the effective surface area of photocatalysts and favors separation of oxidation and reduction centers.

In the present paper we report the results of research on the photocatalytic properties of layered perovskite-like tantalates $ANdTa_2O_7$ (A = H, Li, Na, K, Rb, Cs), their ability of intercalate water into the interlayer space, optical properties, and photocatalytic activity in the reaction of hydrogen evolution from aqueous solutions containing 0.1% of isopropanol. This work is a continuation of research on correlation of the photocatalytic activity of layered oxides and their ability to intercalate water [6, 10].

Complex layered tantalates $ANdTa_2O_7$ belong to the Dion–Jacobson phases [11] and are constructed by a block principle by alternating perovskite-like layers and alkali metal atoms. Depending on the size of the cation in the interlayer space, the perovskite layers can shift by 1/2 the unit cell parameter in the *a* and *b* direction. As a result, oxides crystallize in different structural types (Fig. 1).

For water intercalation studies all samples were ground in an agate mortar and placed into distilled water for 10 h. Oxide suspensions were filtered through a cellulose acetate filter and dried over dehydrated silica to remove traces of surface moisture, after which the samples were subjected to thermogravimetric and X-ray phase analysis.

The $ANdTa_2O_7$ samples (A = Li, K, Rb, Cs) showed no visible changes on contact with water, as evidenced by the observation of no weight losses in the TGA curves (Fig. 2) and by the identity of the X-ray diffraction patterns before and after TGA. The $NaNdTa_2O_7$ and $HNdTa_2O_7$ samples showed about 4% weight losses on heating to 200 and 500°C, respectively. The X-ray diffraction patterns of these samples before and after TGA differ by the positions of the peaks with non-zero l index from the *hkl* set, specifically these peaks shift to larger angles, implying contraction of the crystal lattice in a direction perpendicular to the layer plane. These findings led us to conclude that the investigated samples contain intercalated water that evaporates at 60–500°C.

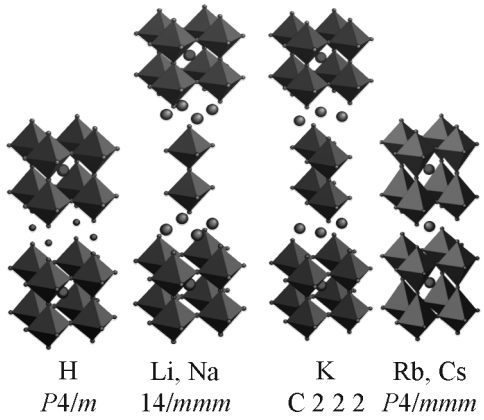

Fig. 1. Structure of perovskite-like tantalates $ANdTa_2O_7$ (A = H, Li, Na, K, Rb, Cs).

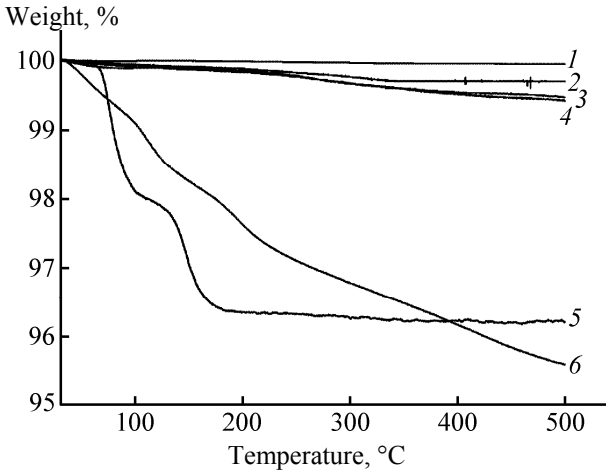

Fig. 2. Thermogravimetric curves of $ANdTa_2O_7$ (A = H, Li, Na, K, Rb, Cs) samples after keeping in water: (*1*) $CsNdTa_2O_7$; (*2*) $LiNdTa_2O_7$; (*3*) $KNdTa_2O_7$; (*4*) $RbNdTa_2O_7$; (*5*) $NaNdTa_2O_7$; and (*6*) $HNdTa_2O_7$.

To obtain evidence for this suggestion, we performed simultaneous thermal analysis (STA) of $NaNdTa_2O_7$ and $HNdTa_2O_7$ combined with mass spectrometry analysis of the evolved gases. As a result, endotherms associated with water evaporation were revealed in the weight loss ranges for both compounds (Figs. 3 and 4).

According to the STA data, the samples lose water in a few stages. To establish the structure of the intermediate compounds, we made X-ray phase analysis after every weight loss stage. The unit cell parameters *c* calculated from these X-ray diffraction patterns, as well as the compositions of the compounds, calculated from the TGA data, are presented in Table 1.

Each of the two weight loss stages of $NaNdTa_2O_7{\cdot}xH_2O$ involves contraction of the crystal lattice perpendicular to the layer plane (Fig. 3). The increase in the lattice parameter in going from anhydrous to hydrated forms occurs irregularly. When 0.6 mol of water is added to 1 mol of anhydrous oxide,

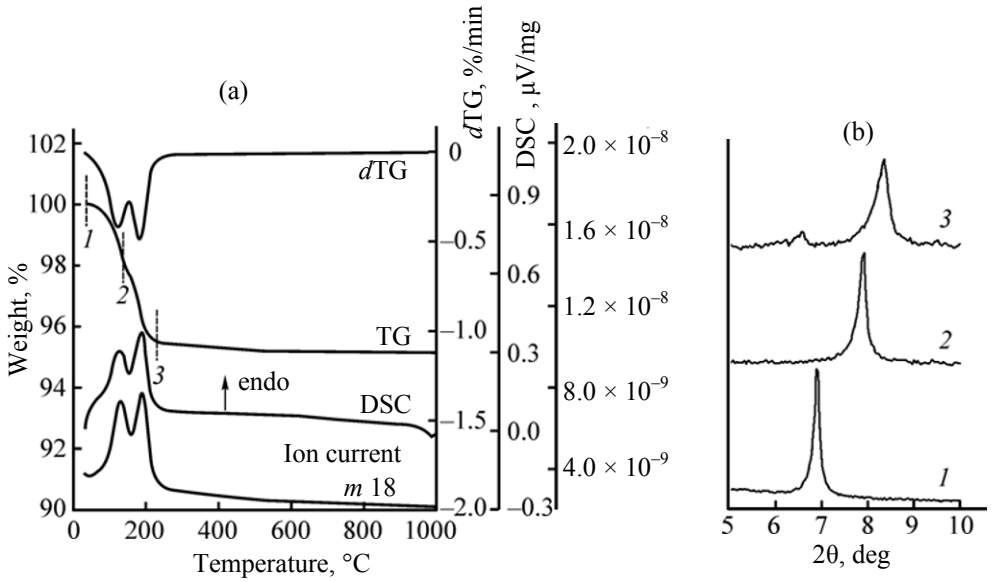

Fig. 3. Results of simultaneous thermal and X-ray phase analysis of $NaNdTa_2O_7$: (a) simultaneous thermal analysis of the intercalate $NaNdTa_2O_7{\cdot}1.35H_2O$ (X-ray phase analysis was performed in points *1–3*); (b) X-ray phase analysis of $NaNdTa_2O_7$ after (*1*) synthesis and heating to (*2*) 105 and (*3*) 170°C.

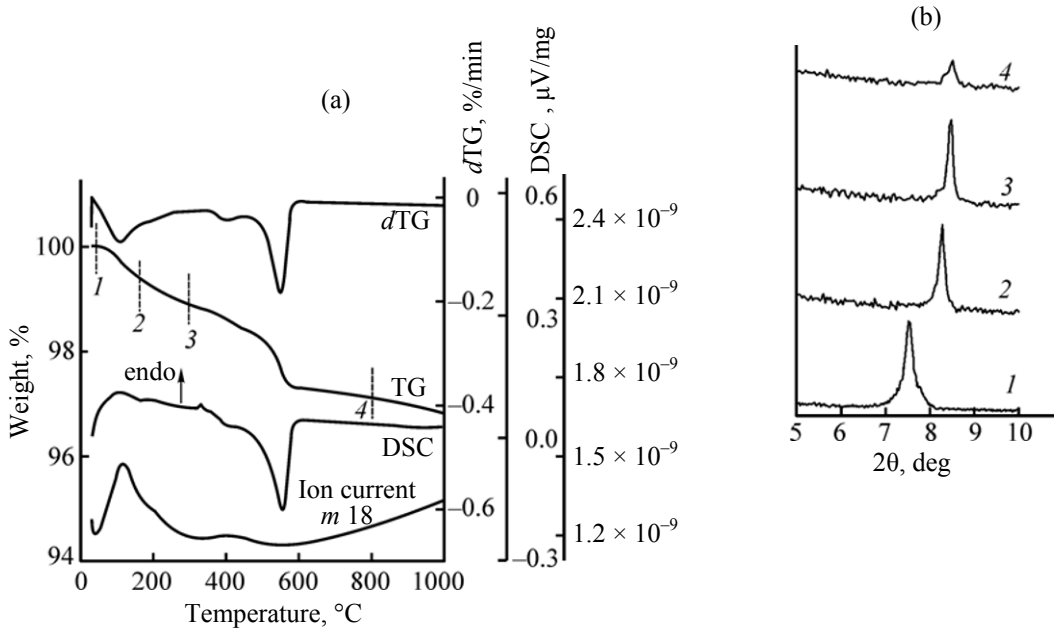

Fig. 4. Results of simultaneous thermal and X-ray phase analysis of $HNdTa_2O_7$: (a) simultaneous thermal analysis of the intercalate $HNdTa_2O_7 \cdot 0.84H_2O$ and $0.25H_2O_s$ (X-ray phase analysis was performed in points *1–4*); (b) X-ray phase analysis of $NaNdTa_2O_7$ after (*1*) synthesis and heating to (*2*) 165, (*3*) 300, and (*4*) 800°C.

the lattice parameter increases by 1.34 Å. Further increase in the quantity of water by 0.75 mol increases the *c* parameter by 3.28 Å.

The weight loss of the $HNdTa_2O_7 \cdot xH_2O$ sample from 30–165 to 165–310°C also results in a decrease in the *c* parameter due to water liberation from the interlayer space. However, further weight loss until 600°C is not accompanied with a change in the *c* parameter. The X-ray diffraction pattern shows a sharp decrease in the intensity of the corresponding peaks, which is characteristic for thermal decomposition of hydrogen forms of layered perovskite-like oxides [12]. Further heating to 1000°C does not lead to weight loss, implying that the decomposition of the solid acid with water evolution completes before 600°C. Therewith, $NdTa_2O_{6.5}$ with a defect perovskite structure and partially preserved layered structure. Thus, the weight loss in the second and third stages allows us to state that $HNdTa_2O_7$ is able to intercalate water in the interlayer space. The weight loss at the first stage (<30°C) corresponds to a loss of 0.25 mol of adsorbed water.

Analysis of the thermogravimetry and differential scanning calorimetry data shows that, unlike $NaNdTa_2O_7 \cdot 1.35H_2O$, the intercalate of the compound with the H^+ cation in the interlayer space does not have a temperature range where the intercalated form $HNdTa_2O_7 \cdot 0.84H_2O$ is partially stable. The observation of a sharp change in the rate of water evolution at 165°C suggests that this is the moment when the stage involving a loss of weakly bound intercalated water to form a thermally more stable form with a smaller quantity of intercalated water in the interlayer space

Table 1. Composition and unit cell parameters of $ANdTa_2O_7$ (A = H, Na) samples at temperatures corresponding to completion of weight loss stages

Chemical formula	Temperature range of stability, °C	Unit cell parameter *c*, Å
$NaNdTa_2O_7 \cdot 1.35H_2O$	<65	25.770
$NaNdTa_2O_7 \cdot 0.60H_2O$	105–125	22.367
$NaNdTa_2O_7$	>170	21.024
$HNdTa_2O_7 \cdot 0.84H_2O_i \cdot 0.25H_2O_s$[a]	<30	11.71
$HNdTa_2O_7 \cdot 0.84H_2O$	<75	11.71
$HNdTa_2O_7 \cdot 0.40H_2O$	165	10.69
$HNdTa_2O_7$	300	10.48
$NdTa_2O_{6.5}$	>600	10.48

[a] (i) Intercalated water; (s) sorbed water.

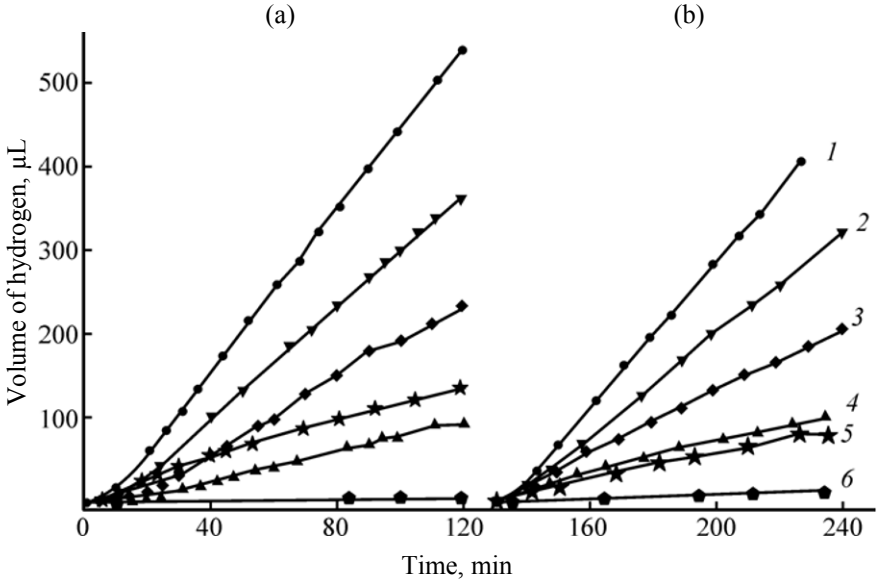

Fig. 5. Dependence of the volume of evolved hydrogen on time of UV irradiation from $ANdTa_2O_7$ suspensions in 0.1% aqueous isopropanol: (*1*) $RbNdTa_2O_7$, (*2*) $CsNdTa_2O_7$, (*3*) $NaNdTa_2O_7$, (*4*) $KNdTa_2O_7$, (*5*) $HNdTa_2O_7$, and (*6*) $LiNdTa_2O_7$. (a) Start of the experiment and (b) after intermediate purging the system with argon.

comes to completion. The stages of water evolution and $HNdTa_2O_7$ decomposition can only be differentiated by a bend on the TGA curve. The characteristic feature of this compound is that the ranges of thermal stability of the intercalate and of the layered oxide are overlapping.

The photocatalytic activity of the $ANdTa_2O_7$ samples was evaluated by measuring the rate of hydrogen evolution from their aqueous suspensions in 0.1% isopropanol under UV irradiation. The kinetic curves obtained in these experiments (Fig. 5) have a constant slope over the entire experiment duration. The rate of hydrogen evolution varies nonmonotonically and increases in the series Li < K < H < Na < Cs < Rb.

Table 2 lists the rates of hydrogen evolution from aqueous suspensions, as well as the measured physicochemical parameters that affect the photocatalytic activity.

Compounds prepared by ion exchange and able to intercalate water ($HNdTa_2O_7 \cdot 0.84H_2O$, $NaNdTa_2O_7 \cdot 1.35H_2O$) show a higher photocatalytic activity. However, tantalates $ANdTa_2O_7$ ($A = H^+$, Li^+, Na^+, and K^+) are difficult to compare, because they not only contain different cations, but also have different structures.

The isostructural compounds $LiNdTa_2O_7$ and $NaNdTa_2O_7 \cdot 1.35H_2O$ have close specific surface areas and bandgap energies. The principal factors responsible for strong differences in the photocatalytic activity are the nature of the interlayer cation and the ability to interacalate water to the oxide structure. The possibility of water intercalation suggests that after the UV-induced decomposition of water in the interlayer space and removal of gaseous products the vacancy that forms is rapidly filled due to water intercalation.

The $RbNdTa_2O_7$ and $CsNdTa_2O_7$ compounds that have the lowest specific surface area show the highest photocatalytic activity. These compounds are unable to intercalate water to the interlayer space and have quite close bandgap energies.

No correlation was found between photocatalytic activity and specific surface area or bandgap energy. Note that the tantalate the most catalytically active among the compounds studied has the lowest specific surface area. There is also no explicit correlation between the photocatalytic activity of layered oxides and their ability to intercalate water to the interlayer space. The effect of the alkali metal on the photocatalytic activity is more likely to be manifested in changes in the structure and structurally sensitive properties of layered oxides. In particular, this effect may be associated with different distortions of the tantalum–oxygen octahedra, which leads to different spacial separations of photogenerated charge carriers [13]. Thus, to explain the different photocatalytic activities of tantalates $ANdTa_2O_7$ (A = H, Li, Na, K,

Table 2. Rates of hydrogen evolution, bandgap energies, and specific surface areas of layered oxides $ANdTa_2O_7$ (A = H, Li, Na, K, Rb, Cs) and their ability to intercalate water

Sample	Rate of hydrogen evolution, μL/h	Bandgap energy E_g, eV	Specific surface area S_{sp}, m^2/g	Water intercalation
$HNdTa_2O_7$	45	4.36	3.9	+
$LiNdTa_2O_7$	6	4.49	4.3	–
$NaNdTa_2O_7$	104	4.38	5	+
$KNdTa_2O_7$	42	4.38	1.2	–
$RbNdTa_2O_7$	263	4.54	0.8	–
$CsNdTa_2O_7$	183	4.40	2	–

Rb, Cs), further research on the structure and electronic structure of these complex oxides is required.

EXPERIMENTAL

Layered perovskite-like oxides $ANdTa_2O_7$ (A = Rb, Cs) were synthesized by the solid-state method from the corresponding simple oxides and carbonates Nd_2O_3 (99.9%), Ta_2O_5 (99.9%), and A_2CO_3 (99.9%). All reagents were calcined before use to remove traces of moisture.

$$Nd_2O_3 + 2Ta_2O_5 + A_2CO_3 \rightarrow 2ANdTa_2O_7 + CO_2\uparrow.$$

The alkali metal carbonate was taken in a 20% excess to compensate its losses during heating. The reagents were weighed with an accuracy of up to 1×10^{-4} g, mixed, and thoroughly ground in an agate mortar for 40 min per 1 g of the mixture. The resulting mixture was pressed into 0.5-g tablets which were placed into a corundum crucible and calcined in a furnace with a silicon carbide heating element at 850°C for 10 h and at 1100°C for 10 h. According to X-ray phase analysis data, all synthesized compounds are single-phase and contain no appreciable impurities.

Compounds $MNdTa_2O_7$ (M = Li, Na, K) could not be synthesized by a standard ceramic procedure, because they are unstable at the high temperatures of synthesis [11]. These compounds were obtained by ion-exchange synthesis by substitution of Rb^+ in $RbNdTa_2O_7$ by Li^+, Na^+, or K^+ in the melts of the corresponding nitrates. Alkali metal nitrates were taken in a 50-fold excess.

Alkali metal nitrate and $RbNdTa_2O_7$ were mixed on a magnetic stirrer (IKA C-MAG HS 7) at 360°C for 10 h. This temperature was chosen taking into account the melting and decomposition points of alkali metal nitrates. The temperature of the reaction mixture was controlled with a thermocouple. The melt was cooled and dissolved in distilled water, and the reaction product was filtered on a cellulose acetate filter (pore diameter 0.22 μm) and dried for 24 h over silica gel.

To prepare $HNdTa_2O_7$, a suspension of 10 mmol of $CsNdTa_2O_7$ in 100 mL of 1N HCl was stirred for 72 h at room temperature. The reaction product was filtered on a cellulose acetate filter and dried for 24 h over silica gel.

The phase composition of the resulting samples and structural changes in the course of the water intercalation–deintercalation process were controlled by an ARL X'TRA powder diffractometer (CuK_α radiation).

The diffuse reflection spectra of complex oxides were measured on a Shimadzu UV-2550 spectrophotometer equipped with an ISR-2200 integrating sphere attachment. The bandgap energy was determined by a standard procedure by constructing the Kubelka–Munk function in the coordinates $(K \cdot h\nu)^{1/2} = f(h\nu)$ and searching for an intersection point of linear parts.

Thermogravimetric analysis was performed on Netzsch TG 209 F1 Libra thermomicrobalance with an accuracy of up to 10^{-7} g; simultaneous thermal analysis (TGA + DSC) combined with mass spectrometry was performed on a Netzsch STA 449 F1 Jupiter instrument with a Netzsch QMS 403C Aeolos quadrupole mass spectrometer.

The kinetics of light-induced hydrogen evolution were studied on the installation described in [6]. A suspension of layered oxide in 0.1% aqueous isopropanol was placed into an external irradiation cell

equipped with a magnetic stirrer. The quantity of evolved hydrogen was measured by gas chromatography. The radiation source was a DRT-125 mercury lamp. Short-wave UV radiation ($\lambda < 220$ nm) was cut off using a light filter containing NaCl and KBr.

ACKNOWLEDGMENTS

The work was performed on the equipment of the Resource Center of Thermal Analysis and Calorimetry, St. Petersburg State University, and was financially supported by the Russian Foundation for Basic Research (project no. 12-03-00761) and St. Petersburg State University (project no. 12.38.257.2014).

REFERENCES

1. Sivakumar, T. and Gopalakrishnan, J., *Mater. Res. Bull*., 2005, vol. 40, no. 1, p. 39. DOI: 10.1016/j.materresbull.2004.09.015.
2. Shimizu, K., Tsuji, Y., Hatamachi, T., Toda, K., Kodama, T., Sato, M., and Kitayama, Y., *Phys. Chem*., 2004, vol. 6, p. 1064. DOI: 10.1039/b312620j.
3. Huang, Y., Li, J., Wei, Y., Li, Y., Lin, J., and Wu, J., *J. Hazard. Mater*., 2009, vol. 166, no. 1, p. 103. DOI: 10.1016/j.jhazmat.2008. 11.040.
4. Huang, Y., Wei, Y., Fan,L., Huang, M., Lin, J., and Wu, J., *Int. J. Hydrogen Energ*., 2009, vol. 34, no. 13, p. 5318. DOI: 10.1016/j.ijhydene.2009.04.040.
5. Rodionov, I.A., Silyukov, O.I., and Zvereva, I.A., *Russ. J. Gen. Chem*., 2012, vol. 82, no. 4, p. 635. DOI: 10.1134/S1070363212040032.
6. Rodionov, I.A., Silyukov, O.I., Utkina, T.D., Chislov, M.V., Sokolova, Y.P., and Zvereva, I.A., *Russ. J. Gen. Chem*., 2012, vol. 82, no. 7, p. 1191. DOI: 10.1134/S1070363212070018.
7. Huang, Y., Li, Y., Wei, Y., Huang, M., and Wu, J., *Sol. Energy Mater. Sol. Cells*, 2011, vol. 95, no. 3, p. 1019. DOI: 10.1016/j.solmat.2010.12.017.
8. Machida, M., Miyazaki, K., Matsushima, S., and Arai, M., *J. Mater. Chem*., 2003, vol. 13, no. 6, p. 1433. DOI: 10.1039/B301938C.
9. Wu, J., Yibin, L., Huang, Y., Huang, M., and Lin, J., *J. Hazard. Mater*., 2010, vol. 177, p. 458. DOI: 10.1016/j.jhazmat.2009. 12.005.
10. Silyukov, O., Chislov, M., Burovikhina, A., Utkina, T., and Zvereva, I., *J. Therm. Anal. Calorim*., 2012, vol. 110, p. 187. DOI: 10.1007/s10973-012-2198-5.
11. Dion, M., Ganne, M., and De Chimie, L., *Mater. Res. Bull*., 1981, vol. 16, no. 11, p. 1429. DOI: 0025-5408/81/111429- 07$02.00/0.
12. Hermann, A.T. and Wiley, J.B., *Mater. Res. Bull*., 2009, vol. 44, no. 5, p. 1046. DOI: 10.1016/j.materresbull.2008.10.019.
13. Mitsuyama, T., Tsutsumi, A., Sato, S., Ikeue, K., and Machida, M., *J. Solid State Chem*., 2008, vol. 181, p. 1419. DOI: 10.1016/j.jssc.2008.03.020.